

Probing the coupling of heavy dark matter to nucleons by detecting neutrino signature from the Earth's core

Guey-Lin Lin, Yen-Hsun Lin, and Fei-Fan Lee

Institute of Physics, National Chiao Tung University, Hsinchu 30010, Taiwan

(Received 23 September 2014; published 5 February 2015)

We argue that the detection of the neutrino signature from the Earth's core can effectively probe the coupling of heavy dark matter ($m_\chi > 10^4$ GeV) to nucleons. We first note that direct searches for dark matter (DM) in such a mass range provide much less stringent constraint than the constraint provided by such searches for $m_\chi \sim 100$ GeV. Furthermore, the energies of neutrinos arising from DM annihilation inside the Sun cannot exceed a few TeVs at the Sun's surface due to the attenuation effect. Therefore, the sensitivity to the heavy DM coupling is lost. Finally, the detection of the neutrino signature from the Galactic halo can only probe DM annihilation cross sections. We present neutrino event rates in IceCube and KM3NeT arising from the neutrino flux produced by annihilation of Earth-captured DM heavier than 10^4 GeV. The IceCube and KM3NeT sensitivities to spin-independent DM-proton scattering cross section $\sigma_{\chi p}$ in this mass range are presented for both isospin-symmetric and isospin-violating cases.

DOI: [10.1103/PhysRevD.91.033002](https://doi.org/10.1103/PhysRevD.91.033002)

PACS numbers: 14.60.Pq, 14.60.St

I. INTRODUCTION

Evidence for dark matter (DM) is provided by many astrophysical observations, although the nature of DM is yet to be uncovered. The most popular candidates for DM are weak interacting massive particles (WIMP), which we shall assume in this work. DM can be detected either directly or indirectly with the former observing the nucleus recoil as DM interacts with the target nuclei in the detector and the latter detecting final state particles resulting from DM annihilation or decays. The direct detection is possible because the dark matter particles constantly bombard the Earth as the Earth sweeps through the local halos. Sensitivities to the DM-nucleon cross section $\sigma_{\chi p}$ from DM direct searches are low for large DM mass m_χ . Given a fixed DM mass density ρ_0 in the solar system, the number density of DM particles is inversely proportional to m_χ . Furthermore, the nuclear form factor suppression is more severe for DM-nucleus scattering for large m_χ . For a review of direct detection, see [1].

In this work, we propose to probe the coupling of heavy DM to nucleons by indirect approach with neutrinos. We note that the flux of DM-induced neutrinos from the Galactic halo is only sensitive to the thermally averaged DM annihilation cross section $\langle\sigma v\rangle$. Furthermore, the energies of neutrinos from the Sun cannot exceed a few TeVs due to severe energy attenuation during the propagation inside the Sun. Hence, for $m_\chi > 10^4$ GeV, we turn to the possibility of probing such DM with the search for the neutrino signature from the Earth's core.

In this paper, we study the neutrino signature from DM annihilation channels $\chi\chi \rightarrow \nu\bar{\nu}$, $\tau^+\tau^-$, and W^+W^- . We do not consider $\chi\chi \rightarrow \mu^+\mu^-$ because muons will suffer severe energy losses in the Earth before they decay to neutrinos.

The soft neutrino spectrum in this case is dominated by the atmospheric background. One also expects that the neutrino telescopes are less sensitive to heavy quark channels such as $\chi\chi \rightarrow b\bar{b}$ than they are to leptonic channels. This is caused by the relatively softer neutrino spectrum resulting from the b -hadron decays compared to the neutrino spectrum from τ decays [2]. For light quark channels $\chi\chi \rightarrow q\bar{q}$, the hadronic cascades produce pions or kaons in large multiplicities. These hadrons decay almost at rest and produce MeV neutrino fluxes. Such fluxes are not considered here since we are interested in the sensitivities of IceCube and KM3NeT, which have much higher threshold energies. However, for detectors aiming at lower-energy neutrinos, such neutrino fluxes might be of interest. For DM annihilation in the Sun, the detectability of such neutrino fluxes has been demonstrated in Refs. [3,4].

The status of the IceCube search for neutrinos coming from DM annihilation in the Earth's core has been reported [5]. The earlier IceCube data on the search for astrophysical muon neutrinos was used to constrain the cross section of DM annihilation $\chi\chi \rightarrow \nu\bar{\nu}$ in the Earth's core [6] for m_χ in the favored range of the PAMELA and Fermi experiments [7,8]. The sensitivity of the IceCube-DeepCore detector to various DM annihilation channels in the Earth's core for low mass DM has also been studied in Ref. [9]. In this work, we shall extend such an analysis to $m_\chi > 10^4$ GeV as mentioned before. We consider both muon track events and cascade events induced by neutrinos in the IceCube observatory. The DM annihilation channels $\chi\chi \rightarrow \tau^+\tau^-$, W^+W^- , and $\nu\bar{\nu}$ will be analyzed. Besides analyzing these signatures in IceCube, we also study the sensitivity of the KM3NeT observatory to the same signature. The KM3NeT observatory [10] is a multi-cubic-kilometer-scale deep sea neutrino telescope to be built in the Mediterranean Sea.

KM3NeT will act as IceCube's counterpart in the northern hemisphere. Because of its instrumental volume of several cubic kilometers, KM3NeT will be the largest and most sensitive water Cherenkov neutrino detector. The sensitivities to DM annihilation cross section $\langle\sigma v\rangle$ and DM-proton scattering cross section $\sigma_{\chi p}$ are expected to be enhanced significantly by KM3NeT.

This paper is organized as follows. In Sec. II, we discuss DM capture and annihilation rates inside the Earth and the resulting neutrino flux. We note that the neutrino flux in this case depends on both the DM annihilation cross section $\langle\sigma v\rangle$ and the DM-proton scattering cross section $\sigma_{\chi p}$. In Sec. III, we discuss the track and cascade event rates resulting from DM annihilation in the Earth's core. The background event rates from the atmospheric neutrino flux are also calculated. In Sec. IV, we compare signature and background event rates and obtain the sensitivities of the neutrino telescopes to the DM-proton scattering cross section. We present those sensitivities in both the isospin-symmetric and isospin-violating [11,12] cases, respectively. We present the summary and conclusion in Sec. V.

II. DARK MATTER ANNIHILATION IN THE EARTH'S CORE

A. DM capture and annihilation rates in the Earth's core

For our interested mass range, $m_\chi > 10^4$ GeV, DM particles are trapped in a small spherical region in the Earth's core, which can be approximated as a point. In fact, the volume of dark matter occupation in the Earth's core is given by $V_\chi(m_\chi) = V_0(20 \text{ GeV}/m_\chi)^{2/3}$ with $V_0 = 2.3 \times 10^{25} \text{ cm}^3$ [13]. For $m_\chi = 10^4$ GeV, the radius for V_χ is only about 100 km. Hence, the neutrino differential flux $d\Phi_{\nu_i}/d\bar{E}_{\nu_i}$ from the annihilation channel $\chi\chi \rightarrow f\bar{f}$ can be expressed as

$$\frac{d\Phi_{\nu_i}}{d\bar{E}_{\nu_i}} = \int dE_{\nu_i} T_{\nu_i}(\bar{E}_{\nu_i}, E_{\nu_i}) \frac{\Gamma_A}{4\pi R_\oplus^2} \sum_f B_f \left(\frac{dN_{\nu_i}}{dE_{\nu_i}} \right), \quad (1)$$

where R_\oplus is the Earth's radius, B_f is the branching ratio of the annihilation channel $\chi\chi \rightarrow f\bar{f}$, dN_{ν_i}/dE_{ν_i} is the energy spectrum of ν_i produced per DM annihilation in the Earth's core, Γ_A is the DM annihilation rate in the Earth, and $T_{\nu_i}(\bar{E}_{\nu_i}, E_{\nu_i})$ summarizes the neutrino propagation effects including attenuation, regeneration, and energy losses from the source to the detector. We stress that the above propagation effects are treated as stochastic processes. The variable E_{ν_i} denotes the neutrino energy at the production point, while \bar{E}_{ν_i} is the neutrino energy at the detector. The integration over E_{ν_i} in Eq. (1) reflects the stochastic nature of neutrino energy loss; i.e., E_{ν_i} and \bar{E}_{ν_i} are not in one-to-one correspondence. In the absence of propagation effects, we have $T_{\nu_i}(\bar{E}_{\nu_i}, E_{\nu_i}) = \delta(\bar{E}_{\nu_i} - E_{\nu_i})$.

In general, $T_{\nu_i}(\bar{E}_{\nu_i}, E_{\nu_i})$ is a smooth function and $\int d\bar{E}_{\nu_i} T_{\nu_i}(\bar{E}_{\nu_i}, E_{\nu_i}) < 1$ is due to the neutrino flux attenuation. To compute $d\Phi_{\nu_i}/d\bar{E}_{\nu_i}$, we employed WIMPSIM [14] so that the neutrino propagation effects summarized by $T_{\nu_i}(\bar{E}_{\nu_i}, E_{\nu_i})$ are fully taken care of.

We note that WIMPSIM only provides the neutrino spectrum dN_{ν_i}/dE_{ν_i} for $m_\chi \leq 10^4$ GeV on its web site. For $m_\chi > 10^4$ GeV, we obtain dN_{ν_i}/dE_{ν_i} by assuming dN_{ν_i}/dZ_i ($Z_i \equiv E_{\nu_i}/m_\chi$) is independent of m_χ . We have verified such an assumption for $10^3 \leq m_\chi/\text{GeV} \leq 10^4$. We further note that the calculation of $T_{\nu_i}(\bar{E}_{\nu_i}, E_{\nu_i})$ is not limited to $m_\chi < 10^4$ GeV in WIMPSIM [15].

Although $T_{\nu_i}(\bar{E}_{\nu_i}, E_{\nu_i})$ can be calculated by WIMPSIM, it is useful to discuss the qualitative features of this function. For $E_\nu \gtrsim 100$ TeV, all flavors of neutrinos interact with nucleons inside the Earth with a total cross section $\sigma \propto E^{0.5}$ [16]. Charged current (CC) and neutral current (NC) neutrino-nucleon interactions occur in the ratio 0.71:0.29, and the resulting lepton carries about 75% of the initial neutrino energy in both cases [16]. For CC interaction, initial ν_e and ν_μ will disappear, and the resulting e and μ will be brought to rest due to their electromagnetic energy losses. Thus, high-energy ν_e and ν_μ are absorbed by the Earth; i.e., CC interaction affects the normalization of $T_{\nu_e}(\bar{E}_{\nu_e}, E_{\nu_e})$ [such as $\int d\bar{E}_{\nu_e} T_{\nu_e}(\bar{E}_{\nu_e}, E_{\nu_e})$] and $T_{\nu_\mu}(\bar{E}_{\nu_\mu}, E_{\nu_\mu})$. However, the situation is very different for ν_τ [17,18] because, except for very high energies ($\gtrsim 10^6$ TeV), the tau lepton decay length is less than its range. Hence, the tau lepton decays in flight without significant energy loss. In every branch of tau decays, ν_τ is produced. In this regeneration process $\nu_\tau \rightarrow \tau \rightarrow \nu_\tau$, the regenerated ν_τ carries about 1/3 of the initial ν_τ energy [19,20]. Those ν_τ arriving at the detector site can be identified through cascade events. Therefore, the functional form rather than the normalization of $T_{\nu_\tau}(\bar{E}_{\nu_\tau}, E_{\nu_\tau})$ is affected by CC interaction. In NC interactions, the initial neutrinos of all flavors are subject to the same energy losses. Hence, the neutrino spectrum of each flavor is shifted to the lower energy range. As a result, only the functional form of $T_{\nu_i}(\bar{E}_{\nu_i}, E_{\nu_i})$ is affected by NC interaction.

The annihilation rate, Γ_A , can be obtained by solving the DM evolution equation in the Earth's core [21,22],

$$\dot{N} = C_C - C_A N^2 - C_E N, \quad (2)$$

where N is the DM number density in the Earth's core, C_C is the capture rate, and C_E is the evaporation rate. The evaporation rate is only relevant when $m_\chi \lesssim 5$ GeV [23–25], while a more refined calculation found, $m_\chi \lesssim 3.3$ GeV [26], which is much lower than our interested mass scale. Thus, C_E can be ignored in this work. The detailed discussion and derivation of the evolution

equation (2) can be found in Refs. [23–27]. Solving Eq. (2), thus, gives the annihilation rate

$$\Gamma_A = \frac{C_C}{2} \tanh^2\left(\frac{t}{\tau_\oplus}\right), \quad (3)$$

where τ_\oplus is the time scale when the DM capture and annihilation in the Earth's core reach the equilibrium state. Taking $t \approx 10^{17}$ s as the lifetime of the solar system, we have [27]

$$\frac{t}{\tau_\oplus} \approx 1.9 \times 10^4 \left(\frac{C_C}{\text{s}^{-1}}\right)^{1/2} \left(\frac{\langle\sigma v\rangle}{\text{cm}^3 \text{s}^{-1}}\right)^{1/2} \left(\frac{m_\chi}{10 \text{ GeV}}\right)^{3/4}, \quad (4)$$

where $\langle\sigma v\rangle$ is the DM annihilation cross section, m_χ is the DM mass, and C_C is the DM capture rate which can be expressed as [27]

$$C_C \propto \left(\frac{\rho_0}{0.3 \text{ GeV cm}^{-3}}\right) \left(\frac{270 \text{ km s}^{-1}}{\bar{v}}\right) \left(\frac{\text{GeV}}{m_\chi}\right) \times \left(\frac{\sigma_{\chi p}}{\text{pb}}\right) \sum_i F_{A_i}(m_\chi), \quad (5)$$

where ρ_0 is the local DM density, \bar{v} is the DM velocity dispersion, $\sigma_{\chi p}$ is the DM-nucleon cross section, and $F_{A_i}(m_\chi)$ is the product of various factors for element A_i , including the mass fraction, chemical element distribution, kinematic suppression, form factor, and reduced mass. We note that $\sigma_{\chi p}$ is spin independent in the Earth's case. We also point out that the factors F_{A_i} behave as $1/m_\chi$ when m_χ is much heavier than the nucleus mass m_{A_i} . Thus, the mass dependence of the capture rate goes as $1/m_\chi^2$.

B. Isospin violation effects to bounds set by direct and indirect searches

Recent studies [11,12,28,29] suggested that DM-nucleon interactions do not necessarily respect the isospin symmetry. It has been shown that [12,29,30] isospin violation can dramatically change the bound on $\sigma_{\chi p}$ from the current direct search. Therefore, the isospin violation effect is also taken into consideration in our analysis.

Given an isotope with atomic number Z , atom number A_i , and the reduced mass $\mu_{A_i} \equiv m_\chi m_{A_i}/(m_\chi + m_{A_i})$ for the isotope and the DM particle, the usual DM-nucleus cross section with the approximation $m_p \approx m_n$ can be written as [27]

$$\begin{aligned} \sigma_{\chi A_i} &= \frac{4\mu_{A_i}^2}{\pi} [Zf_p + (A_i - Z)f_n]^2 \\ &= \frac{\mu_{A_i}^2}{\mu_p^2} \left[Z + (A_i - Z) \frac{f_n}{f_p} \right]^2 \sigma_{\chi p}, \end{aligned} \quad (6)$$

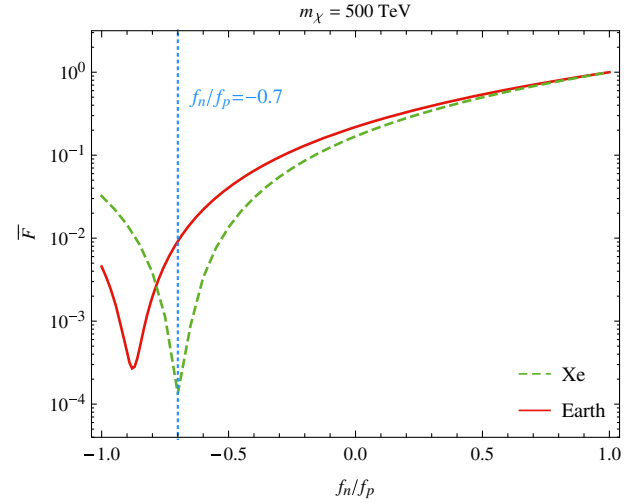


FIG. 1 (color online). Isospin violation effect versus f_n/f_p for different targets at $m_\chi = 500$ TeV. For the Xenon target, \bar{F} reduces to F_Z . In this case, F_Z reaches a minimum at $f_n/f_p = -0.7$. With the Earth as the target, $\bar{F} \equiv \sum_Z f_Z F_Z$ where f_Z is the fraction of proton targets originating from chemical elements with the atomic number Z . In this case, \bar{F} reaches a minimum for $f_n/f_p \approx -0.9$. We have taken the Earth's composition from Ref. [27]. The fraction f_Z is taken as the average fraction of a chemical species inside the Earth.

where f_p and f_n are the effective couplings of DM to protons. It is useful to define the ratio between $\sigma_{\chi A_i}^0$ and $\sigma_{\chi A_i}$ where the former is the DM-nucleus cross section assuming isospin symmetry and the latter is the cross section with isospin violation. In this ratio, the DM-proton cross section $\sigma_{\chi p}$ is held fixed. For a particular species of chemical element with atomic number Z , we have

$$\frac{\sigma_{\chi A_i}^0}{\sigma_{\chi A_i}} = \frac{\sum_i \eta_i \mu_{A_i}^2 A_i^2}{\sum_i \eta_i \mu_{A_i}^2 [Z + (A_i - Z) f_n/f_p]^2} \equiv F_Z, \quad (7)$$

where η_i is the percentage of the isotope A_i . We note that for a target containing multiple species of chemical elements, the factor F_Z should be modified into $\bar{F} \equiv \sum_Z f_Z F_Z$, where f_Z is the fraction of proton targets originating from elements with the atomic number Z . Figure 1 shows the numerical values of \bar{F} versus different f_n/f_p at $m_\chi = 500$ TeV. Since m_χ is taken to be much larger than m_{A_i} , \bar{F} is insensitive to m_χ .

III. DM SIGNAL AND ATMOSPHERIC BACKGROUND EVENTS

The neutrino event rate in the detector resulting from DM annihilation in the Earth's core is

$$N_\nu = \int_{E_{\text{th}}}^{E_{\text{max}}} \frac{d\Phi_\nu}{dE_\nu} A_\nu(E_\nu) dE_\nu d\Omega, \quad (8)$$

where E_{th} is the detector threshold energy taken to be 10^4 GeV, E_{max} is the energy upper cut, and $d\Phi_\nu/dE_\nu$ is the neutrino flux from DM annihilation. As neutrinos arrive at the detector, they interact with the medium enclosed by the detector and produce track events through ν_μ CC interaction. Cascade events are produced via $\nu_{e,\tau}$ CC and all ν_i NC interactions. The quantity A_ν is the detector effective area with contained vertex and Ω is the solid angle for the event direction. Given the sizes of IceCube and KM3NeT, we take $E_{\text{max}} = 10^7$ GeV.

As seen from the detector, the DM-induced neutrino flux comes from a small angular range surrounding the direction to the center of the Earth. The solid angle $\Delta\Omega$ subtended by the cross sectional area of the DM-populated region V_χ is given by $\Delta\Omega = 2\pi(1 - \cos\psi_\chi)$ with ψ_χ given by [9]

$$\psi_\chi(m_\chi) = \sin^{-1} \left[\frac{1}{R_\oplus} \times \left(\frac{3V_\chi(m_\chi)}{4\pi} \right)^{1/3} \right]. \quad (9)$$

For $m_\chi = 10^4$ GeV, we have $\psi_\chi = 0.9^\circ$. Hence, ψ_χ is always less than 1° in our interested DM mass range. Ideally, one may select neutrino events by setting the observation open angle, $\psi = \psi_\chi(m_\chi)$. However, due to the detector angular resolution, we choose the open angle, $\psi = 1^\circ$, for track events and $\psi = 30^\circ$ for cascade events to reflect the current IceCube performance [31,32].

In this work, we consider neutrino events in neutrino detectors IceCube and KM3NeT. To compute the event rates in IceCube, the effective areas A_ν for different neutrino flavors with CC and NC interactions in Eq. (8) can be evaluated from the effective volume V_{eff} [31] by the following relation,

$$A_\nu(E_\nu) = V_{\text{eff}} \frac{N_A}{M_{\text{ice}}} (n_p \sigma_{\nu p}(E_\nu) + n_n \sigma_{\nu n}(E_\nu)), \quad (10)$$

where N_A is the Avogadro constant, M_{ice} is the molar mass of ice, $n_{p,n}$ is the number density of proton/neutron per mole of ice, and $\sigma_{\nu p,n}$ is the neutrino-proton/neutron cross section. One simply swaps the sign $\nu \rightarrow \bar{\nu}$ for the antineutrino.

We note that another neutrino telescope KM3NeT located in the northern hemisphere is also capable of detecting the neutrino signal from DM annihilation in the Earth. At the present stage, KM3NeT has only published the ν_μ CC effective area [10,32]. Therefore, we consider only track events in KM3NeT.

The atmospheric background event rate is similar to Eq. (8) by replacing $d\Phi_\nu/dE_\nu$ with the atmospheric neutrino flux,

$$N_{\text{atm}} = \int_{E_{\text{th}}}^{E_{\text{max}}} \frac{d\Phi_\nu^{\text{atm}}}{dE_\nu} A_\nu(E_\nu) dE_\nu d\Omega. \quad (11)$$

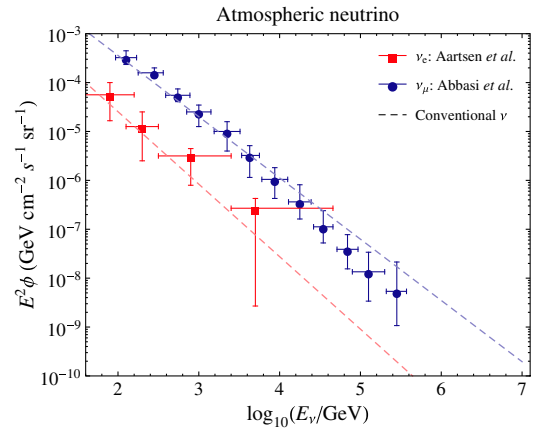


FIG. 2 (color online). The atmospheric ν_e and ν_μ flux.

To facilitate our calculation, the atmospheric neutrino flux $d\Phi_\nu^{\text{atm}}/dE_\nu$ shown in Fig. 2 is taken from Refs. [33,34] and extrapolated to $E_\nu \approx 10^7$ GeV.

IV. RESULTS

We present the sensitivity as a 2σ detection significance in five years, calculated with the convention

$$\frac{s}{\sqrt{s+b}} = 2.0, \quad (12)$$

where s is the DM signal, b is the atmospheric background, and 2.0 refers to the 2σ detection significance. The atmospheric ν_τ flux is extremely small and can be ignored in our analysis. Thus, we take ν_e and ν_μ as our major background sources. The detector threshold energy E_{th} in Eqs. (8) and (11) is set to be 10^4 GeV in order to suppress the background events. In the following two subsections, we present two isospin scenarios for the constraints on $\langle\sigma v\rangle$ and $\sigma_{\chi p}$. One is $f_n/f_p = 1$, the isospin-symmetry case, and the other is $f_n/f_p = -0.7$, the isospin-violation one. The isospin-violation scenario is often used to alleviate the inconsistency between the results of different DM direct detection experiments for low m_χ . The ratio $f_n/f_p = -0.7$ is the value for which the $\sigma_{\chi p}$ sensitivity of a Xenon detector is maximally suppressed by isospin violation. Although our study focuses on heavy DM accumulated inside the Earth and Xenon is very rare among the constituent elements of the Earth, we shall see that $f_n/f_p \sim -0.7$ leads to the most optimistic IceCube sensitivities on both $\langle\sigma v\rangle$ and $\sigma_{\chi p}$. In the next subsection, we present various f_n/f_p values and their impact on the IceCube sensitivities to various annihilation channels.

To derive sensitivities to the DM-annihilation cross section $\langle\sigma v\rangle$, we make use of the $\sigma_{\chi p}$ from the extrapolation of the LUX bound [35] to $m_\chi > 10$ TeV. Such an input $\sigma_{\chi p}$ represents the best scenario in our analysis. Once a more

stringent bound on $\sigma_{\chi p}$ is obtained in the future, the sensitivities to $\langle\sigma v\rangle$ presented in this work will be worse.

The extrapolation of the LUX bound to our interested m_χ range can be justified as follows. The total rate R measured by the direct search is given by $R \propto \sigma_{\chi p} \rho_0 / m_\chi m_{A_i}$ for $m_\chi \gg m_{A_i}$ [27], with ρ_0 the local DM density, m_{A_i} the mass of the target, and i the index for isotopes. Thus, $\sigma_{\chi p} \propto m_\chi m_{A_i} R / \rho_0$. Hence, the linear extrapolation of the LUX bound in the mass range $m_\chi > 10$ TeV is reasonable.

A. IceCube sensitivities

In Fig. 3 we present the IceCube sensitivities to $\langle\sigma v\rangle$ of $\chi\chi \rightarrow \tau^+\tau^-$, W^+W^- , and $\nu\bar{\nu}$ annihilation channels in the Earth's core with both track and cascade events. For the $\chi\chi \rightarrow \nu\bar{\nu}$ production mode, we assume equal-flavor distribution (1/3 for each flavor). In the left panel where $f_n = f_p$, the IceCube sensitivities to $\chi\chi \rightarrow \tau^+\tau^-$ and $\chi\chi \rightarrow W^+W^-$ annihilation channels with track events are only available in a narrow DM mass range. For most of the DM mass range considered here, the estimated sensitivities are either disfavored by the CMB constraint or reach into the equilibrium region where the 2σ sensitivity cannot be achieved. The raising tails for all sensitivities are due to the neutrino attenuation in the high energy such that larger $\langle\sigma v\rangle$ is required to generate sufficient number of events.

For $m_\chi \gtrsim 10^6$ GeV, it is seen that IceCube is more sensitive to $\chi\chi \rightarrow \tau^+\tau^-$ than to $\chi\chi \rightarrow \nu\bar{\nu}$ for cascade events. This can be understood by the fact that the neutrino spectrum from $\chi\chi \rightarrow \nu\bar{\nu}$ is almost like a spike near m_χ . As m_χ becomes larger, neutrinos produced by the annihilation are subject to more severe energy attenuation. On the other hand, the neutrino spectrum from $\chi\chi \rightarrow \tau^+\tau^-$ is

relatively flat in the whole energy range. The energy attenuation only affects the higher energy neutrinos.

In the isospin violation scenario, the ratio $f_n/f_p = -0.7$ reduces the scattering cross section between DM and Xenon by 4 orders of magnitude with a fixed $\sigma_{\chi p}$. This is easily seen from Fig. 1. Hence, the LUX upper bound on $\sigma_{\chi p}$ is raised by 4 orders of magnitude. With the same f_n/f_p ratio, one can also see that the DM capture rate by the Earth is suppressed by 2 orders of magnitude. If one takes the LUX upper bound on $\sigma_{\chi p}$ for $f_n/f_p = -0.7$ as the input, the capture rate C_C of the Earth is enhanced by 2 orders of magnitude. One can estimate the enhancement on the neutrino flux by Eq. (3). We note that the number of DM particles inside the Earth is still far from the equilibrium, i.e., $\tanh(t/\tau_\oplus) \approx t/\tau_\oplus$. Hence, we can see that Γ_A is proportional to $C_C^2 \langle\sigma v\rangle$ by using Eq. (4). This is rather different from the equilibrium case where Γ_A is proportional to C_C . Since C_C is 2 orders of magnitude larger for $f_n/f_p = -0.7$, the bound on $\langle\sigma v\rangle$ derived from Γ_A is improved by 4 orders of magnitude.

For DM produced as a thermal relic of the big bang, the DM relic density Ω_χ is related to the thermally averaged annihilation cross section $\langle\sigma v\rangle$ by [27]

$$\Omega_\chi h^2 \approx \frac{3 \times 10^{-27} \text{ cm}^3 \text{ s}^{-1}}{\langle\sigma v\rangle}. \quad (13)$$

By substituting $\Omega_\chi h^2$ for $\mathcal{O}(0.1)$ in the present epoch, we have $\langle\sigma v\rangle \approx 3 \times 10^{-26} \text{ cm}^3 \text{ s}^{-1}$, which is known as the thermal relic scale. We note that Eq. (13) is a simplified relation ignoring its dependence on the WIMP mass. With the mass dependence treated carefully, one obtains $\langle\sigma v\rangle \approx (2-5) \times 10^{-26} \text{ cm}^3 \text{ s}^{-1}$ for $\Omega_\chi h^2 = 0.11$ [37]. We should

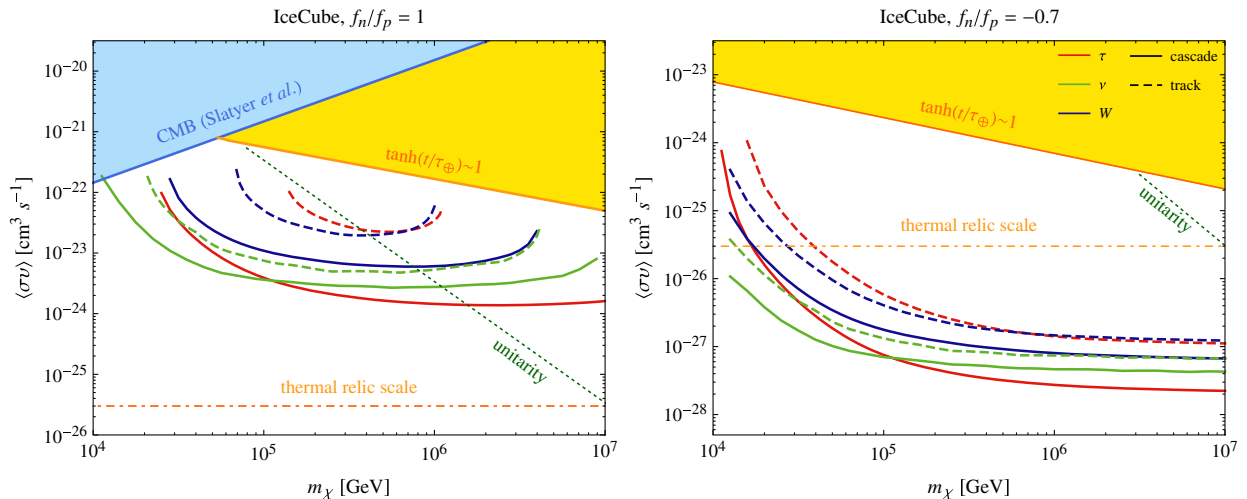


FIG. 3 (color online). The IceCube five-year sensitivities at 2σ to $\langle\sigma v\rangle$ for $\chi\chi \rightarrow \tau^+\tau^-$, W^+W^- , and $\nu\bar{\nu}$ annihilation channels with track and cascade events. We take $\psi = 1^\circ$ for track events and $\psi = 30^\circ$ for cascade events. The isospin-symmetry case, $f_n/f_p = 1$, is presented in the left panel, and the isospin-violation case, $f_n/f_p = -0.7$, is presented in the right panel. The yellow-shaded region is the parameter space for the equilibrium state, and the blue-shaded region is the constraint from CMB [36].

point out that the DM in our considered mass range could be produced nonthermally. In such a case, there is no canonical value for $\langle\sigma v\rangle$. However, $\langle\sigma v\rangle$ is bounded from the above by the unitarity condition [38–40]. The DM annihilation cross section is assumed to be s -wave dominated in the low-velocity limit. Hence, it can be shown that [38]

$$\langle\sigma v\rangle \leq \frac{4\pi}{m_\chi^2 v} \approx 1.5 \times 10^{-13} \frac{\text{cm}^3}{\text{s}} \left(\frac{\text{GeV}}{m_\chi}\right)^2 \left(\frac{300 \text{ km/s}}{v_{\text{rms}}}\right). \quad (14)$$

This unitarity bound with $v_{\text{rms}} \approx 13 \text{ km s}^{-1}$ (escape velocity from the Earth) is also shown in Fig. 3. The unitarity bound can be evaded for nonpointlike DM particles [39–41].

Galaxy clusters (GCs) are the largest gravitationally bound objects in the Universe, and their masses can be as large as 10^{15} times that of the Sun's ($10^{15} M_\odot$) [42,43]. Many galaxies (typically ~ 50 – 1000) collect into GCs, but their masses consist of mainly dark matter. Thus, GCs are the largest DM reservoirs in the Universe and can be the ideal sources to look for DM annihilation signatures. With DM particles assumed to annihilate into $\mu^+\mu^-$ pairs, the predicted full IceCube 2σ sensitivity in five years to $\langle\sigma v\rangle$ for the Virgo cluster in the presence of substructures with track events is derived in Ref. [44]. We present this sensitivity in Fig. 4, and we can see that it is better than our expected IceCube five-year sensitivity at 2σ to $\langle\sigma(\chi\chi \rightarrow \tau^+\tau^-)v\rangle$ with ν_μ track events. One of the reasons is because only 18% of τ decay to ν_μ . However, if we consider the isospin-violation scenario, our expected IceCube sensitivity with $f_n/f_p = -0.7$ will be much better than that for the Virgo cluster. Except for neutrinos, DM annihilation in GCs can also produce a high luminosity in gamma rays. In Ref. [44], the authors also estimate gamma-ray constraints taking into account electromagnetic cascades caused by pair production on the cosmic photon backgrounds from the flux upper limits derived by Fermi-LAT observations of GCs [45,46]. We show in Fig. 4 the gamma-ray constraint on the $\chi\chi \rightarrow \mu^+\mu^-$ annihilation cross section [44] from observations of the Virgo cluster. We can see that this constraint is weaker than our expected IceCube five-year sensitivity at 2σ to $\langle\sigma(\chi\chi \rightarrow \tau^+\tau^-)v\rangle$ for $m_\chi \gtrsim 10^5 \text{ GeV}$. We note however that the constraint on $\langle\sigma v\rangle$ from the Virgo cluster is independent of $\sigma_{\chi p}$, while our expected sensitivity with $\sigma_{\chi p}$ taken from the LUX bound represents the best scenario. If we reevaluate our expected sensitivity by using smaller $\sigma_{\chi p}$, the results could be weaker than the constraint from the Virgo cluster.

The diffuse gamma-ray background (DGB) was measured by the Fermi Large Area Telescope (Fermi-LAT) above 200 MeV in 2010 [47]. Radio-loud active galactic nuclei (AGN), including blazars [48], star-forming and

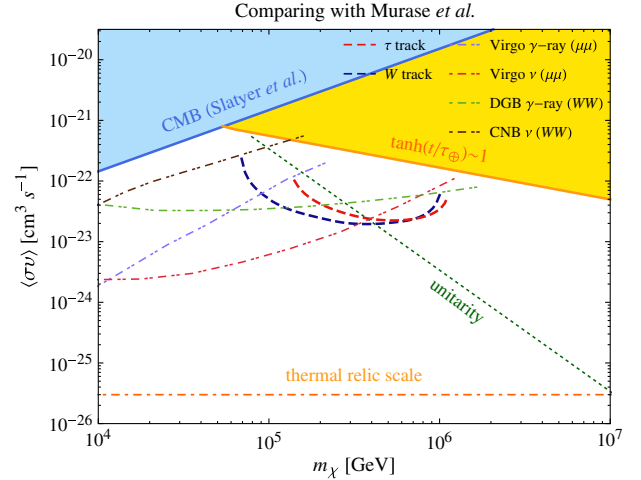


FIG. 4 (color online). The IceCube five-year sensitivities at 2σ to $\langle\sigma v\rangle$ for $\chi\chi \rightarrow W^+W^-$ and $\tau^+\tau^-$ annihilation channels with track events. We take $\psi = 1^\circ$. The dot-dashed line is the gamma-ray constraint on the $\chi\chi \rightarrow \mu^+\mu^-$ annihilation cross section in the Virgo cluster [44]. The dashed line is the projected full IceCube 2σ sensitivity in five years to $\langle\sigma(\chi\chi \rightarrow \mu^+\mu^-)v\rangle$ in the Virgo cluster in the presence of substructures with track events [44]. The dot-dot-dashed line is the cascade gamma-ray constraint on $\langle\sigma(\chi\chi \rightarrow W^+W^-)v\rangle$ from diffuse gamma-ray background (DGB) [41]. The thick solid line is the full IceCube sensitivity in three years to $\langle\sigma(\chi\chi \rightarrow W^+W^-)v\rangle$ from cosmic neutrino background (CNB) with track events [41].

star-burst galaxies [49,50], and heavy DM are the possible sources. In Ref. [41], the authors derive cascade gamma-ray constraints on the annihilation cross section of heavy DM by requiring that the calculated cascade gamma-ray flux not exceed the measured DGB data at any individual energy bin by more than a given significance [51,52]. We present the cascade gamma-ray constraint on $\langle\sigma(\chi\chi \rightarrow W^+W^-)v\rangle$ for DGB taken from Ref. [41] in Fig. 4. We note that this constraint is weaker than our predicted IceCube five-year sensitivity at 2σ to $\langle\sigma(\chi\chi \rightarrow W^+W^-)v\rangle$. On the other hand, for demonstrating the power of neutrino observations, we also show in Fig. 4 the predicted full IceCube sensitivity in three years to $\langle\sigma(\chi\chi \rightarrow W^+W^-)v\rangle$ for the cosmic neutrino background (CNB) with track events taken from Ref. [41]. It is slightly less sensitive compared to our expected IceCube five-year sensitivity at 2σ to $\langle\sigma(\chi\chi \rightarrow W^+W^-)v\rangle$ at $m_\chi \sim 10^5 \text{ GeV}$, while both sensitivities do not reach the unitarity bound for $m_\chi \gtrsim 3 \times 10^5 \text{ GeV}$. We reiterate that our derived sensitivity to $\langle\sigma(\chi\chi \rightarrow W^+W^-)v\rangle$ is the best-scenario result, while constraints obtained in Ref. [41] are independent of $\sigma_{\chi p}$.

Figure 5 shows the IceCube sensitivities to spin-independent cross section $\sigma_{\chi p}$ by analyzing track and cascade events from $\chi\chi \rightarrow \tau^+\tau^-$, W^+W^- , and $\nu\bar{\nu}$ annihilation channels in the Earth's core. The threshold energy E_{th} is the same as before, and we take $\langle\sigma v\rangle = 3 \times 10^{-26} \text{ cm}^2 \text{ s}^{-1}$ as our input. Precisely speaking, the

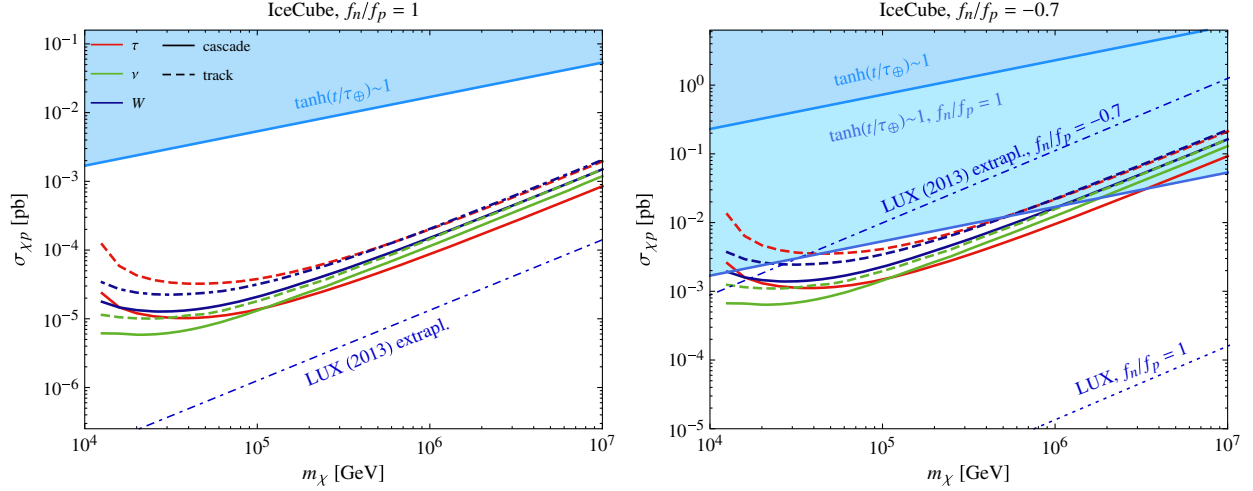


FIG. 5 (color online). The IceCube 2σ sensitivities in five years to $\sigma_{\chi p}$ for $\chi\chi \rightarrow \tau^+\tau^-$, W^+W^- , and $\nu\bar{\nu}$ annihilation channels with both track ($\psi = 1^\circ$) and cascade events ($\psi = 30^\circ$). The isospin symmetry case, $f_n/f_p = 1$, is presented on the left, and the isospin violation case, $f_n/f_p = -0.7$, is presented on the right. The blue-shaded region is the parameter space for the equilibrium state and the light-blue-shaded region in the right panel refers to the equilibrium-state parameter space for the isospin symmetry case as a comparison. An extrapolation of current LUX limit has been shown on the figures.

sensitivity to the $\chi\chi \rightarrow \nu\bar{\nu}$ channel is the highest when $m_\chi \lesssim 10^6$ GeV and $\chi\chi \rightarrow \tau^+\tau^-$ after. However, the sensitivities to different channels can be taken as comparable since the differences between them are not significant.

When the isospin is a good symmetry, the IceCube sensitivity is not as good as the constraint from the LUX extrapolation. However, with $f_n/f_p = -0.7$, the capture rate is reduced to 1% of the isospin symmetric value. Therefore, one requires 100 times larger $\sigma_{\chi p}$ to reach the same detection significance. However, the ratio $f_n/f_p = -0.7$ makes a more dramatic impact to the DM direct search using Xenon as the target. The DM scattering cross

section with Xenon is reduced by 4 orders of magnitude. Hence, the indirect search by IceCube could provide better sensitivities on $\sigma_{\chi p}$ than the direct search in such a case.

B. KM3NeT sensitivities

Besides IceCube, the neutrino telescope KM3NeT located in the northern hemisphere can also reach a promising sensitivity in the near future [53]. Therefore, it is worthwhile to comment on the performance of KM3NeT. Since KM3NeT has only published the ν_μ CC

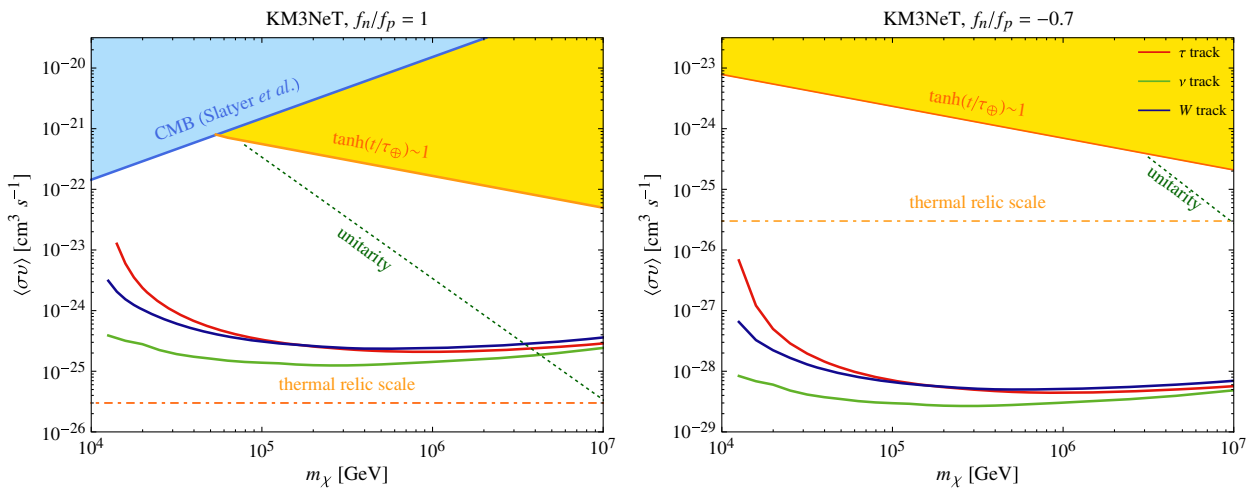


FIG. 6 (color online). The KM3NeT 2σ sensitivities in five years to $\langle\sigma v\rangle$ for $\chi\chi \rightarrow \tau^+\tau^-$, W^+W^- , and $\nu\bar{\nu}$ annihilation channels for track events with $\psi = 1^\circ$. The isospin symmetry case, $f_n/f_p = 1$, is presented in the left panel, and the isospin violation case, $f_n/f_p = -0.7$, is presented in the right panel. The yellow-shaded region is the parameter space for the equilibrium state and the blue-shaded region is the constraint from CMB [36].

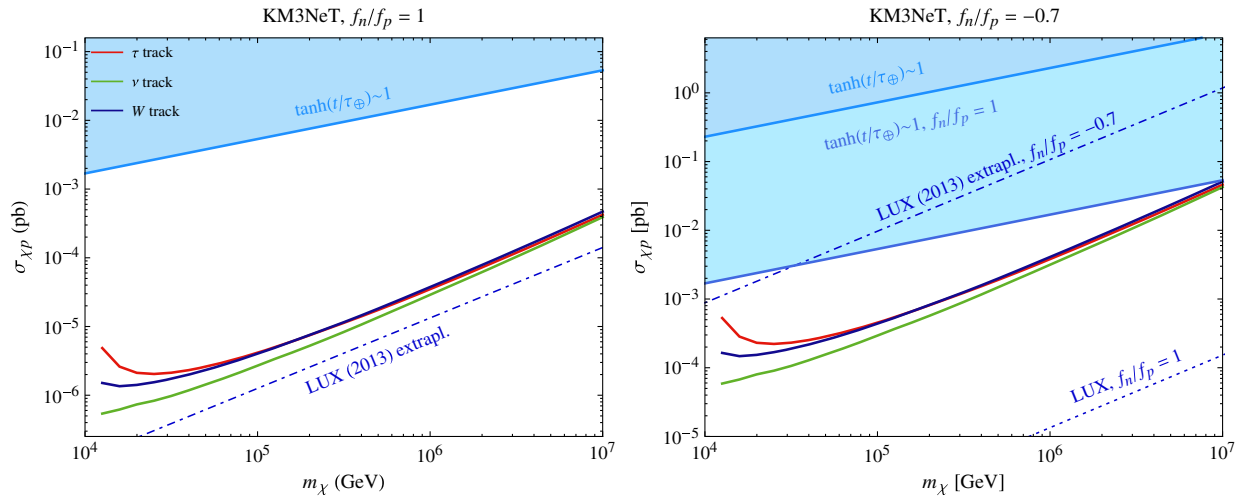


FIG. 7 (color online). The KM3NeT 2σ sensitivities in five years to $\sigma_{\chi p}$ for $\chi\chi \rightarrow \tau^+\tau^-$, W^+W^- , and $\nu\bar{\nu}$ annihilation channels for track events with $\psi = 1^\circ$. The isospin symmetry case, $f_n/f_p = 1$, is presented in the left panel, and the isospin violation case, $f_n/f_p = -0.7$, is presented in the right panel. The blue-shaded region is the parameter space for the equilibrium state, and the light-blue-shaded region in the right panel refers to the equilibrium-state parameter space in the isospin-symmetry case.

effective area [10] at the present stage, we shall only analyze track events.

The results are shown in Figs. 6 and 7 with parameters chosen to be the same as those for computing the IceCube sensitivities. The sensitivities of KM3NeT are almost an order of magnitude better than those of IceCube, since its ν_μ CC effective area is about 1 order of magnitude larger than that of IceCube.

C. Sensitivities with different f_n to f_p ratios

In the previous subsections, we have presented IceCube and KM3NeT sensitivities to $\langle\sigma v\rangle$ and $\sigma_{\chi p}$ for $f_n/f_p = 1$ and -0.7 . To be thorough, it is worth discussing the effect

on the DM search with various f_n/f_p values. For simplicity, we shall focus on the $\chi\chi \rightarrow \tau^+\tau^-$ cascade events in IceCube.

In the left panel of Fig. 8, we present IceCube sensitivities to $\langle\sigma v\rangle$ with $f_n/f_p \in [-0.8, 1]$. We take the rederived $\sigma_{\chi p}$ from LUX using Eq. (7), which quantifies the isospin violation effect. Isospin violation not only leads to the suppression of the DM capture rate by the Earth but also weakens the $\sigma_{\chi p}$ bound from LUX. The overall effect favors the DM indirect search for a certain range of f_n/f_p . As shown in Fig. 8, the IceCube sensitivity to $\langle\sigma v\rangle$ improves as $f_n/f_p \rightarrow -0.7$ from the above. However, when f_n/f_p is smaller than -0.7 , the sensitivity to $\langle\sigma v\rangle$

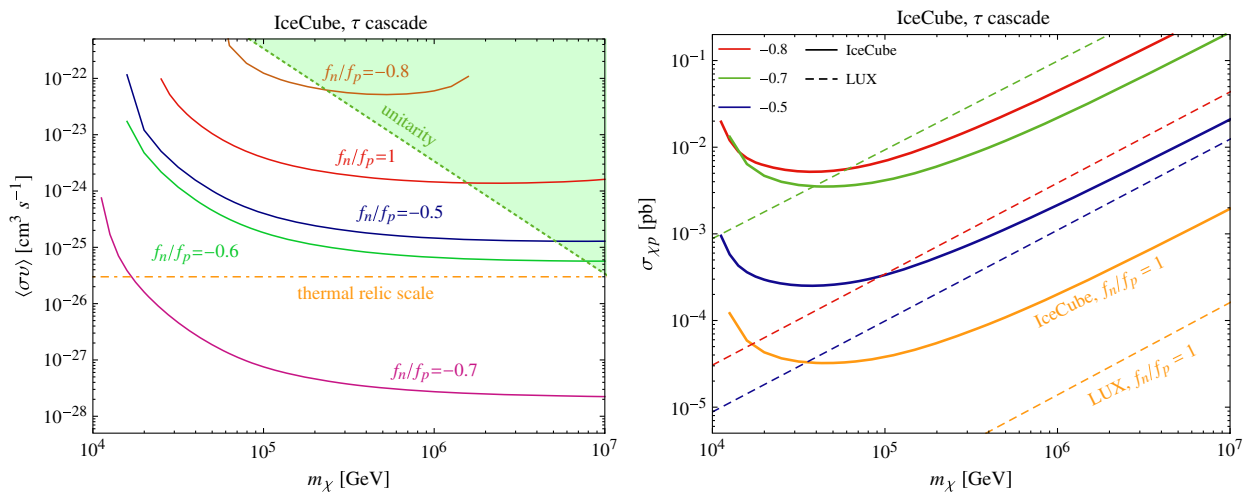


FIG. 8 (color online). The IceCube five-year sensitivity at 2σ to $\langle\sigma v\rangle$ in the left panel and $\sigma_{\chi p}$ in the right panel for $\chi\chi \rightarrow \tau^+\tau^-$ annihilation channels with cascade events for different degrees of isospin violation. We take the rederived $\sigma_{\chi p}$ from LUX with isospin violation taken into consideration.

becomes even worse than that in the isospin-symmetry case.

In the right panel of Fig. 8, we present IceCube sensitivities to $\sigma_{\chi p}$ with $f_n/f_p \in [-0.8, 1]$ by taking $\langle\sigma v\rangle = 3 \times 10^{-26} \text{ cm}^3 \text{ s}^{-1}$ as our input. With isospin symmetry violated, the DM capture rate is suppressed by the factor \bar{F} defined right below Eq. (7). Thus, to reach the same detection significance by indirect search, one requires a larger $\sigma_{\chi p}$ to produce enough events. However, isospin violation also weakens the LUX limit at a certain range of f_n/f_p . It turns out the sensitivity to $\sigma_{\chi p}$ by IceCube is better than the existing limit by LUX only for f_n/f_p slightly larger or equal to -0.7 . For $f_n/f_p < -0.7$, the LUX limit is more stringent.

V. SUMMARY AND CONCLUSION

In this work we have presented the IceCube and KM3NeT sensitivities to thermally averaged annihilation cross section $\langle\sigma v\rangle$ and DM spin-independent cross section $\sigma_{\chi p}$ for heavy DM ($m_\chi > 10^4 \text{ GeV}$) by detecting the DM-induced neutrino signature from the Earth's core. To probe the former, we take $\sigma_{\chi p}$ from the LUX bound [35] as the input. To probe the latter, we take $\langle\sigma v\rangle = 3 \times 10^{-26} \text{ cm}^3 \text{ s}^{-1}$ as the input. The IceCube sensitivity to $\langle\sigma(\chi\chi \rightarrow W^+W^-)v\rangle$ in the present case is slightly better than its sensitivity to $\langle\sigma(\chi\chi \rightarrow W^+W^-)v\rangle$ in the case of detecting the cosmic neutrino background [41]. On the other hand, the IceCube sensitivity to $\langle\sigma(\chi\chi \rightarrow \tau^+\tau^-)v\rangle$

in the present case is not as good as its sensitivity to $\langle\sigma(\chi\chi \rightarrow \mu^+\mu^-)v\rangle$ in the case of detecting neutrinos from the Virgo cluster [44]. We like to emphasize again that our derived sensitivity to $\langle\sigma(\chi\chi \rightarrow W^+W^-)v\rangle$ uses the current LUX bound on $\sigma_{\chi p}$ as the input. One expects this sensitivity to become worse as the constraint on $\sigma_{\chi p}$ improves. Concerning IceCube and KM3NeT sensitivities to $\sigma_{\chi p}$, we have shown that they are roughly 1 order of magnitude worse than the LUX bound.

We stress that the above comparison is based upon the assumption of isospin symmetry in DM-nucleon couplings. We have shown that, like the direct search, the indirect search is also affected by the isospin violation. The implications of isospin violation for IceCube and KM3NeT observations are presented in Sec. IV. Taking the isospin-violation effect into account, the sensitivities of the above neutrino telescopes to both $\langle\sigma v\rangle$ and $\sigma_{\chi p}$ through detecting the signature of DM annihilation in the Earth's core can be significantly improved. As $f_n/f_p \rightarrow -0.7$, the sensitivities to $\langle\sigma v\rangle$ can be better than the thermal relic scale, while the sensitivities to $\sigma_{\chi p}$ can be better than the LUX bound.

ACKNOWLEDGMENTS

We thank Y.-L. Sming Tsai for helpful advice in computations. This work is supported by the National Science Council of Taiwan under Grant No. 102-2112-M-009-017.

-
- [1] P. Cushman, C. Galbiati, D. N. McKinsey, H. Robertson, T. M. P. Tait, D. Bauer, A. Borgland, B. Cabrera *et al.*, [arXiv:1310.8327](https://arxiv.org/abs/1310.8327).
 - [2] The spectral shapes of neutrinos from DM annihilations are summarized in M. Cirelli, G. Corcella, A. Hektor, G. Hutsi, M. Kadastik, P. Panci, M. Raidal, F. Sala, and A. Strumia, *J. Cosmol. Astropart. Phys.* **03** (2011) 051; **10** (2012) E01.
 - [3] C. Rott, J. Siegal-Gaskins, and J. F. Beacom, *Phys. Rev. D* **88**, 055005 (2013).
 - [4] N. Bernal, J. Martn-Albo, and S. Palomares-Ruiz, *J. Cosmol. Astropart. Phys.* **08** (2013) 011.
 - [5] J. Kunnen *et al.* (IceCube Collaboration), Proc. of the 33rd ICRC, Rio de Janeiro, 2013.
 - [6] I. F. M. Albuquerque, L. J. Beraldo e Silva, and C. Perez de los Heros, *Phys. Rev. D* **85**, 123539 (2012).
 - [7] O. Adriani *et al.* (PAMELA Collaboration), *Phys. Rev. Lett.* **106**, 201101 (2011).
 - [8] M. Ackermann *et al.* (Fermi LAT Collaboration), *Phys. Rev. D* **82**, 092004 (2010).
 - [9] F.-F. Lee, G.-L. Lin, and Y.-L. S. Tsai, *Phys. Rev. D* **89**, 025003 (2014).
 - [10] KM3NeT Technical Design Report, <http://km3net.org/TDR/TDRKM3NeT.pdf>.
 - [11] A. Kurylov and M. Kamionkowski, *Phys. Rev. D* **69**, 063503 (2004).
 - [12] J. L. Feng, J. Kumar, D. Marfatia, and D. Sanford, *Phys. Lett. B* **703**, 124 (2011).
 - [13] V. Berezhinsky, A. Bottino, J. R. Ellis, N. Fornengo, G. Mignola, and S. Scopel, *Astropart. Phys.* **5**, 333 (1996).
 - [14] M. Blennow, J. Edsjö, and T. Ohlsson, *J. Cosmol. Astropart. Phys.* **01** (2008) 021.
 - [15] J. Edsjö (private communication).
 - [16] R. Gandhi, C. Quigg, M. H. Reno, and I. Sarcevic, *Astropart. Phys.* **5**, 81 (1996); *Phys. Rev. D* **58**, 093009 (1998).
 - [17] S. Ritz and D. Seckel, *Nucl. Phys.* **B304**, 877 (1988).
 - [18] F. Halzen and D. Saltzberg, *Phys. Rev. Lett.* **81**, 4305 (1998).
 - [19] S. I. Dutta, M. H. Reno, and I. Sarcevic, *Phys. Rev. D* **62**, 123001 (2000).
 - [20] T. K. Gaisser, *Cosmic Rays and Particle Physics* (Cambridge University Press, Cambridge, England, 1992).

- [21] K. A. Olive, M. Srednicki, and J. Silk, Report No. UMN-TH-584/86.
- [22] M. Srednicki, K. A. Olive, and J. Silk, *Nucl. Phys.* **B279**, 804 (1987).
- [23] A. Gould, *Astrophys. J.* **321**, 571 (1987).
- [24] L. M. Krauss, M. Srednicki, and F. Wilczek, *Phys. Rev. D* **33**, 2079 (1986).
- [25] M. Nauenberg, *Phys. Rev. D* **36**, 1080 (1987).
- [26] K. Griest and D. Seckel, *Nucl. Phys.* **B283**, 681 (1987); [**B296**, 1034(E) (1988)].
- [27] G. Jungman, M. Kamionkowski, and K. Griest, *Phys. Rep.* **267**, 195 (1996).
- [28] F. Giuliani, *Phys. Rev. Lett.* **95**, 101301 (2005).
- [29] S. Chang, J. Liu, A. Pierce, N. Weiner, and I. Yavin, *J. Cosmol. Astropart. Phys.* **08** (2010) 018.
- [30] Y. Gao, J. Kumar, and D. Marfatia, *Phys. Lett. B* **704**, 534 (2011).
- [31] M. G. Aartsen *et al.* (IceCube Collaboration), *Science* **342**, 1242856 (2013).
- [32] U. F. Katz (KM3NeT Collaboration), *Nucl. Instrum. Methods Phys. Res., Sect. A* **626–627**, S57 (2011).
- [33] M. G. Aartsen *et al.* (IceCube Collaboration), *Phys. Rev. Lett.* **110**, 151105 (2013).
- [34] M. Honda, T. Kajita, K. Kasahara, S. Midorikawa, and T. Sanuki, *Phys. Rev. D* **75**, 043006 (2007).
- [35] D. S. Akerib *et al.* (LUX Collaboration), *Phys. Rev. Lett.* **112**, 091303 (2014).
- [36] T. R. Slatyer, N. Padmanabhan, and D. P. Finkbeiner, *Phys. Rev. D* **80**, 043526 (2009).
- [37] G. Steigman, B. Dasgupta, and J. F. Beacom, *Phys. Rev. D* **86**, 023506 (2012).
- [38] J. F. Beacom, N. F. Bell, and G. D. Mack, *Phys. Rev. Lett.* **99**, 231301 (2007).
- [39] K. Griest and M. Kamionkowski, *Phys. Rev. Lett.* **64**, 615 (1990).
- [40] L. Hui, *Phys. Rev. Lett.* **86**, 3467 (2001).
- [41] K. Murase and J. F. Beacom, *J. Cosmol. Astropart. Phys.* **10** (2012) 043.
- [42] G. M. Voit, *Rev. Mod. Phys.* **77**, 207 (2005).
- [43] A. Diaferio, S. Schindler, and K. Dolag, *Space Sci. Rev.* **134**, 7 (2008).
- [44] K. Murase and J. F. Beacom, *J. Cosmol. Astropart. Phys.* **02** (2013) 028.
- [45] A. Pinzke, C. Pfrommer, and L. Bergstrom, *Phys. Rev. D* **84**, 123509 (2011).
- [46] M. Ackermann *et al.* (Fermi-LAT Collaboration), *Astrophys. J.* **717**, L71 (2010).
- [47] A. A. Abdo *et al.* (Fermi-LAT Collaboration), *Phys. Rev. Lett.* **104**, 101101 (2010).
- [48] K. N. Abazajian, S. Blanchet, and J. P. Harding, *Phys. Rev. D* **84**, 103007 (2011).
- [49] B. D. Fields, V. Pavlidou, and T. Prodanovic, *Astrophys. J.* **722**, L199 (2010).
- [50] A. Loeb and E. Waxman, *J. Cosmol. Astropart. Phys.* **05** (2006) 003.
- [51] A. A. Abdo *et al.* (Fermi-LAT Collaboration), *J. Cosmol. Astropart. Phys.* **04** (2010) 014.
- [52] M. Ackermann *et al.* (Fermi-LAT Collaboration), *Astrophys. J.* **761**, 91 (2012).
- [53] S. Biagi (KM3NeT Collaboration), *J. Phys. Conf. Ser.* **375**, 052036 (2012).